Korean J. Chem. Eng., **29**(2), 190-195 (2012)
DOI: 10.1007/s11814-011-0160-z

Characterization of chars made of solvent extracted coals

Wan-taek Cho, Sangdo Kim, Ho-kyung Choi, Young-joon Rhim, Jeong-hwan Lim, Si-hyun Lee, and Jiho Yoo†

Climate Change Technology Division, Korea Institute of Energy Research,
102, Gajeong-ro, Yuseong-gu, Daejeon 305-343, Korea
(*Received 14 March 2011 • accepted 14 June 2011*)

Abstract–Thermal extraction of a sub-bituminous coal (Roto south) using 1-methylnaphthalene solvent has produced ash-free coals successfully. The extracted (EC) and residual coal (RC) as well as its parent coal (PC) were pyrolyzed at 300-900 °C and then the carbonized products were characterized. The extracted coal (EC) contained lower molecular weight components than PC and RC, showing much higher fuel ratio after the pyrolysis. EC is expected to be advantageous over PC and RC when applied to coal gasification and reforming, because EC is readily decomposed and volatized. The heating value of EC chars (7,610-8,120 kcal/kg) was independent of the pyrolysis temperature and was higher than those of PC and RC chars, especially for the chars carbonized below 600 °C. The oxygen content of PC chars at T≤600 °C was mostly at least twice that of EC/RC chars, pointing out the difference in the chemical composition. ^{13}C-NMR and FT-IR spectra revealed the release of aliphatic hydrocarbons and reactive functional groups with increasing temperature, in agreement with ultimate/proximate analysis results.

Key words: Coal Char, Ash-free Coal, Low Rank Coal, Solvent Extraction, Carbonization

INTRODUCTION

Coal, one of the most important energy sources, currently accounts for ~25% of worldwide energy consumption [1,2]. The use of coal is expected to increase, thanks to its abundance and economic advantage. However, there are various problems resulting from the combustion of coal such as ash deposition, emission of pollutants and greenhouse gases.

Ash in coal decreases the power efficiency and discharges as an air pollutant [3-5]. Therefore, many works have concentrated on the preparation of ash-free coals [6-17]. Among them, thermal extraction with organic solvents has produced ash-free coals, namely "Hypercoal", most successfully, potentially solving the ash problem [18, 19]. Economically, ash-free coals derived from low rank coals are even more attractive [20].

Recently, ash-free coals have found new applications in direct coal-fired gas turbine, direct carbon fuel cell (DCFC), catalytic gasification, coke additive for iron making industry, and aluminum anode coke, mainly owing to their ashless character and high thermoplasticity [21-24]. The devolatilization of relatively small organic molecules happens in the initial stage of coal utilization. This early devolatilization is influential in the subsequent homogeneous and heterogeneous reactions of char. Therefore, understanding the carbonization characteristics of the extracted coal will be valuable for the practical purpose.

The devolatilization properties of raw coals have been extensively studied, including the structural/compositional transformation (the size of aromatic rings, the nature of functional groups and cross-links), and thermoproperty [25-27]. Alonso et al. found strong dependence of char reactivity on the pyrolysis temperature [28]. Partially carbonized samples in the thermoplastic stage of coking (290-630 °C) were also characterized [29]. However, only limited information is available on the characteristics of chars made of the solvent extracted coal and its insoluble by-product.

In this study the solvent extracted coal was pyrolyzed in the temperature range, 300-900 °C, as well as its insoluble by-product (residual coal) and a parent coal (an Indonesian Roto south sub-bituminous coal). The effect of pyrolysis temperature was analyzed by comparing with one another, based on the data obtained using ultimate/proximate analysis, BET, solid-state ^{13}C-NMR, FT-IR, and XRD.

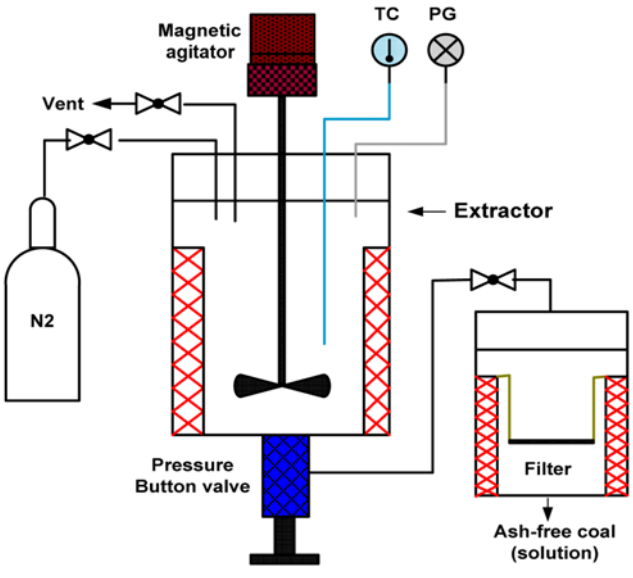

Fig. 1. Schematic diagram of solvent extraction (PG: pressure gauge, TC: thermocouple).

†To whom correspondence should be addressed.
E-mail: jyoo@kier.re.kr

EXPERIMENTAL

1. Preparation of Ashless Coal (Solvent Extraction)

The organic portion of a subbituminous coal (Indonesian Roto south coal) was thermally extracted using non-polar 1-methylnaphthalene (1-MN) solvent. As shown in Fig. 1, the extraction was processed via extraction, filtration, and drying step. A batch-type autoclave (0.5 liter volume) was adapted as an extractor. The raw coal was ground, meshed to <74 μm (200 mesh), and then dried in a vacuum oven. Coal slurry was prepared by combining 20 g of the dried coal with 200 g of 1-MN. The slurry was added to the autoclave, which was then purged with N_2 gas. While stirring with the magnetic agitator, the coal/solvent mixture was heated to 370 °C and held for an hour under 30 bar. The thermally treated sample was transferred to the stainless steel filtering unit to separate the solvent extract from the residual matter. The solvent in both the extract and the residue was removed by being kept in a vacuum oven (~300 °C) for 3-4 hr under N_2 atmosphere, giving solid materials, namely, extracted coal (EC) and residual coal (RC), respectively.

Proximate/ultimate analysis, calorific value, BET surface area of the parent coal (PC), EC, and RC are tabulated in Table 1. Based on ASTM D3172 standard, the proximate analysis determined the content of moisture, ash, volatile matter, and fixed carbon, using TGA-701 Thermogravimeter (LECO Co., USA). Elemental composition (C, H, N, and O) was obtained using CHN-2000 Elemental Analyzer (LECO Co., USA), calorific value using Parr 1261 Calorimeter (PARR Co., USA), and BET surface area using ASAP 2420 (Micromeritics Co., USA).

2. Preparation of Char

The pyrolysis of the samples (PC, EC, and RC) was carried out at 300, 400, 500, 600, 700, 800, and 900 °C. The sample (~5 g) was heated at 10 °C/min ramp rate and kept at the predetermined peak temperature for 30 min under N_2 sweep gas, which prevented coal oxidation and removed the pyrolyzed material from the reaction zone. The product was then naturally cooled to room temperature. Chars of PC, EC, and RC were named as PCC, ECC, and RCC, respectively. The name of the original chars (PCC, ECC, and RCC) was then combined with the pyrolysis temperature; for example, 'ECC-600' corresponds to the char made of EC by 600 °C pyrolysis.

3. Solid-state ^{13}C CP/MAS NMR, FT-IR, and XRD

Solid-state ^{13}C nuclear magnetic resonance (NMR) was performed using the CP/MAS NMR spectrometer (400 MHz, Bruker II+ model, Avance co.). The measurements were made at the carbon frequency =100.62 MHz. About 70 mg of sample was loaded in a sample rotor. All the spectra were acquired, employing contact time of 2 ms, repetition time of 3 sec, and 90° ^{1}H pulse width of 3.8 μs. This was combined with a magic angle-spinning frequency of 13.5 kHz. The chemical shifts were calibrated with respect to tetramethylsilane (TMS) using the peak of the methyl group on hexamethyl-benzene as the external standard.

The chemical functional groups were detected by FT-IR (Nicolet 6700, Thermo Elentron co.). The spectra were measured at 4,000-650 cm^{-1}. X-ray diffraction pattern was obtained using DMAX-2500 (Rigaku co.).

RESULTS AND DISCUSSION

1. Proximate/Ultimate Analysis and Calorific Values

The proximate analysis data of the pyrolyzed PC, EC, and RC are given in Table 2. The ash content of PCC and RCC increased as the pyrolysis temperature increased. The ash content of PCC changed from 2.6 wt% for the raw coal to 5.9 wt% after the carbonization

Table 1. Proximate/ultimate analysis, calorific value, BET surface area of the parent coal (PC), extracted coal (EC), and residual coal (RC)

Sample	Proximate analysis (wt%)				Ultimate analysis (wt%, daf*)				BET (m^2/g)	Calorific value (kcal/kg)
	Moisture	Volatile matter (daf)	Ash (dry)	Fixed carbon (daf)	C	H	N	O		
Parent coal (PC)	7.4	59.0	2.6	41.0	69.0	4.3	0.3	26.4	3.9	5,950
Extracted coal (EC)	-	33.6	<0.1	66.4	87.9	4.3	0.0	7.9	0.2	8,160
Residual coal (RC)	-	39.5	4.6	60.5	87.7	4.2	0.0	8.0	4.1	7,490

*Daf: dry, ash free

Table 2. Results of proximate analysis and calorific values of pyrolyzed PC, EC, and RC

	Ash (wt%, dry)			Volatile matter (wt%, daf*)			Fixed carbon (wt%, daf)			Fuel ratio			Calorific value (kcal/kg)		
T (°C)	PCC	ECC	RCC	PCC	ECC	RCC	PCC	ECC	RCC	PCC	ECC	RCC	PCC	ECC	RCC
300	2.0	0.0	4.7	52.6	32.0	34.5	47.4	68.0	65.5	0.9	2.1	1.9	6020	7610	7330
400	2.9	0.0	4.9	50.6	24.8	32.1	49.4	75.2	67.9	1.0	3.0	2.1	6150	7820	7350
500	3.7	0.0	5.3	49.0	24.3	32.5	51.0	75.7	67.5	1.0	3.1	2.1	6120	7940	7390
600	3.9	0.0	6.7	37.5	16.4	26.4	62.5	83.6	73.6	1.7	5.1	2.8	6910	8020	7410
700	4.8	0.0	7.2	23.3	16.4	22.2	76.7	83.6	77.8	3.3	5.1	3.5	7490	8120	7430
800	4.9	0.0	7.8	19.4	11.4	18.7	80.5	88.6	81.3	4.2	7.8	4.4	7520	7960	7480
900	5.9	0.0	7.9	17.7	8.9	15.3	82.3	91.1	84.7	4.6	10.2	5.6	7430	7980	7520

*Daf: dry, ash free

Table 3. Results of ultimate analysis of pyrolyzed PC, EC, and RC

	C (wt%, daf*)			H (wt%, daf)			N (wt%, daf)			O (wt%, daf)			H/C, O/C		
T	PCC	ECC	RCC	PCC	ECC	RCC	PCC	ECC	RCC	PCC	ECC	RCC	PCC	ECC	RCC
300	70.8	84.1	84.2	3.3	3.9	3.4	0.2	0.0	0.1	25.6	12.0	12.3	0.05, 0.36	0.05, 0.14	0.04, 0.15
400	72.6	87.0	85.1	3.6	3.8	3.3	0.2	0.0	0.3	23.5	9.3	11.3	0.05, 0.32	0.04, 0.11	0.04, 0.13
500	73.4	87.3	85.8	2.4	2.2	2.0	0.5	0.0	0.4	23.7	10.5	10.7	0.03, 0.32	0.03, 0.12	0.02, 0.12
600	82.1	91.5	89.0	2.5	2.0	2.2	0.8	0.0	0.7	14.6	6.5	8.1	0.03, 0.18	0.02, 0.07	0.02, 0.09
700	92.7	93.9	91.7	1.3	1.2	1.4	0.8	0.0	0.7	5.2	4.9	6.1	0.01, 0.06	0.01, 0.05	0.01, 0.07
800	93.6	93.2	93.0	0.8	0.5	0.8	0.5	0.3	0.4	5.1	5.9	5.7	0.01, 0.05	0.01, 0.06	0.01, 0.06
900	93.7	94.6	95.5	0.6	0.6	0.6	0.2	0.2	0.1	5.4	4.6	3.8	0.01, 0.06	0.01, 0.05	0.01, 0.04

*Daf: dry, ash free

at 900 °C. For residual coal (RC), the ash content increased from 4.6 wt% before pyrolysis to 7.9 wt% after heat treatment at 900 °C. This increase resulted from the enrichment of ash due to the loss of volatile matters by raising the temperature. As expected, most of ashes in PCC were retained in RCC during the solvent extraction, and the ash content in ECC was less than 0.1 wt%, regardless of the temperature.

Much higher content of volatile matter in PCC than in ECC and RCC as prepared (Table 1) seemed to be attributed to devolatilization that happened during the solvent drying step at 300 °C. With a rise in the carbonization temperature, a marked decrease in volatile matter along with an increase in fixed carbon content was observed for all three chars (Table 2), leading to an increase of fuel ratio (fixed carbon wt%/volatile matter wt%). The change was most significant at 500-600 °C for ECC and at 500-700 °C for PCC and RCC. EC is more susceptible to devolatilization than RC, since EC has more light components (low molecular weight) readily decomposed and volatized at the elevated temperatures [20]. Much higher fuel ratio of ECC than PCC and RCC agrees with the above idea. More than 65% of the volatiles for PCC and ECC and ~50% for RCC were released by heating at 900 °C, compared to the chars made at 300 °C.

The calorific value of PCC increased notably by heating at 500-700 °C, from 6,120 kcal/Kg for PCC-500 to 7,490 kcal/Kg for PCC-700. Negligible changes were, however, shown at the other temperatures. The abrupt increase seemed to be due to a decrease of oxygen content and a simultaneous increase in carbon content. As shown in Table 3, data of the elemental analysis indicated that the oxygen content was reduced from 23.7 wt% at PCC-500 to 5.2 wt% at PCC-700. It has been known that the calorific value of the oxidized coals is lower than that of the counterpart [30]. The oxygen content in ECC and RCC was less than 50% of PCC chars at T≤600 °C, probably due to the loss of oxygenated groups during the thermal extraction process. Accordingly, relatively small change in the oxygen content and therefore weak temperature dependence of the calorific value were found for ECC and RCC, showing 7,610-8,120 kcal/Kg for ECC and 7,330-7,520 kcal/Kg for RCC. The heating value of ECC was higher than that of PCC and RCC, especially for the chars carbonized below 600 °C, partly as a result of its lower ash and oxygen content [30,31].

In common, the carbon content increased by raising the heating temperature (Table 3), while the hydrogen and oxygen content decreased. No difference in the nitrogen content was observed during the temperature variation. In addition, 0.01-0.1 wt% of sulfur remained in the chars and its content was independent of the pyrolysis conditions (data are not shown). A decrease of the hydrogen content occurred stepwise for all the chars; the hydrogen loss at 500 °C probably corresponded to devolatilization of alkyl groups and that at 700 °C to condensation of the aromatic molecules [31,32]. Regardless of the samples, the oxygen was most likely released by decomposition of oxygen containing functional group such as carboxylic and etheric group, which was significant on 600-700 °C pyrolysis. The carbonized products retained 4-6% oxygen, a typical oxygen level of bituminous coals, when pyrolyzed above 700 °C.

The H/C ratio of the three chars and its temperature dependence were very similar to each other in spite of the different elemental composition (Table 3). The H/C ratio varied from 0.04-0.05 at 300 °C to 0.01 at 900 °C, decreasing gradually with an increase of the pyrolysis temperature. The O/C ratio of PCC obtained at T≤600 °C was at least twice as large as that of ECC and RCC, indicating the difference in the chemical composition [18]. The pyrolysis at the higher temperature (T≥700 °C) devolatilized the majority of the oxygenated groups in PCC, giving about the same level of O/C ratio as in ECC and RCC.

2. BET

The specific surface area of ECC increased enormously when pyrolyzed at 500 °C (Table 4). The BET surface area of ECC-500 was more than two orders of magnitude higher than that of ECC-400. The abrupt change was followed by small change at 600-800 °C. On the other hand, an increase of the BET surface area in PCC and RCC was gradational at the temperature range, 400-700 °C and 300-600 °C, respectively (Table 4). The extracted coal is known to exhibit fluid-like high thermoplasticity at 200-500 °C, accompanying relaxation of the coal structure [20]. The sudden increase in ECC-500 seemed to be due to the thermoplastic deformation (swelling and

Table 4. BET surface area of pyrolyzed PC, EC, and RC

	BET surface area (m^2/g)		
T	PCC	ECC	RCC
300	2.0	0.4	5.7
400	2.1	0.9	30.4
500	83.9	373.3	140.5
600	195.6	390.7	378.2
700	489.8	304.9	380.9
800	467.5	410.7	389.7

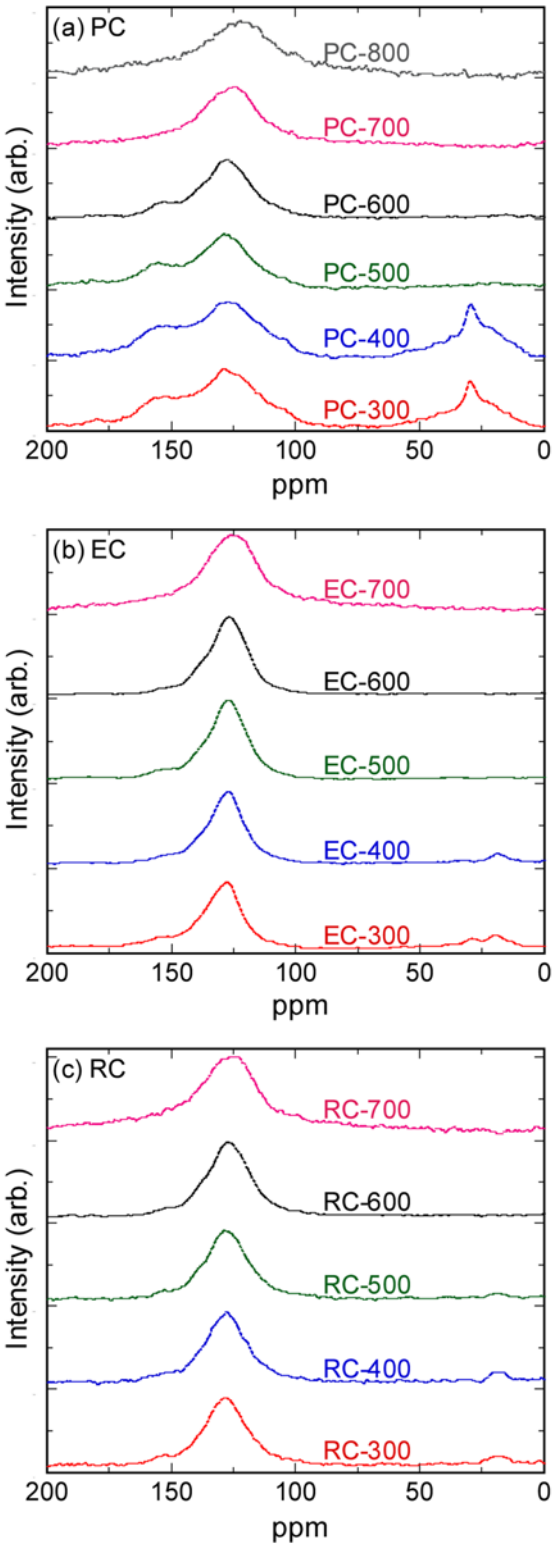

Fig. 2. ^{13}C-NMR spectra of chars made of (a) PC, (b) EC, and (c) RC.

popping) leading to formation of cracks [28]. Temperature dependence of the BET in PCC and RCC was weak at <500 °C, compared to that in ECC, which was probably attributable to their relatively low thermoplasticity. The temperature region showing the considerable BET increment was extended to 700 °C for PCC and to 600 °C for RCC. At the higher temperature, release of volatile matters and resulting formation of pores probably contributed to the BET increase [33,34]. The specific surface area is one of the most influential factors controlling the reaction profile by governing the mass transport behavior. Therefore, both ECC and RCC looked promising as a fuel for direct carbon fuel cell, as it preserved the high surface area at the elevated temperature.

2. Solid-state ^{13}C-NMR

The ^{13}C-NMR spectra of the chars made of PC, EC, and RC are shown in Fig. 2. The NMR spectra revealed the presence of a variety of carbon types and also estimated the ratio of aromatic and aliphatic carbon [35-38]. A weak peak appeared at chemical shift (δ)= 190-175 ppm, a characteristic peak of carboxylic carbons, for PCC-300 and PCC-400 in (a), but disappeared when heat-treated at the higher temperature. That peak was absent for both ECC ((b)) and RCC ((c)) at all the temperatures.

Phenolic carbon peak showed up at δ=165-150 ppm. A phenolic peak was stronger in PCC than in ECC and RCC. For all the samples the intensity became weaker with a temperature increase, such that it disappeared at T≥700 °C. A broad peak covering 150-100 ppm was generally the strongest with the maximum positioned at ~128 ppm. This peak corresponds to the overlap of non-protonated (148-129 ppm) and protonated (129-93 ppm) aromatic carbon peaks [36,37]. The protonated peaks in PCC were strong, compared to those in ECC and RCC.

Intense peaks at δ=50-0 ppm were shown for PCC-300 and PCC-400, whose intensity was comparable to the intensity of their aromatic components ((a)). Much smaller peaks were detected for ECC and RCC at the same condition ((b) and (c)). The peaks at 50-25 ppm can be assigned to unsaturated aliphatic carbons. The peaks in the 25-0 ppm region are due to the resonance of methyl groups attached either to straight-chain aliphatic groups or aromatic/alicyclic structures [35]. The strongest peak in PCC-300 and PCC-400 was found at ~31 ppm and known to be related to the methylenic carbon [35]. A lack of aliphatic peaks in ECC and RCC was most likely caused by the severe solvent evaporation (300 °C for 3-4 hr), indicating that the aliphatic molecules were devolatilized at a lower temperature than any other aromatic species [29]. The aromaticity of the three samples increased with increasing temperature, in agreement with the ultimate analysis results (an increase in carbon content coupled with a decrease in hydrogen content).

3. FT-IR and XRD

The FT-IR spectra of ECC are shown in Fig. 3. The IR profile of PCC and RCC was about the same as that of ECC. Major functional groups were identified in the spectra and labeled accordingly. The numbers in the figure indicate the pyrolysis temperature. Various absorption of oxygenated functional groups were detected such as a weak hydroxyl peak at ~3,500 cm^{-1}, a carbonyl peak at ~1,720 cm^{-1}, and an etheric peak at ~1,250 cm^{-1}. A peak at ~1,610 cm^{-1} corresponded to an aromatic ring stretch, whose intensity was known to be significantly affected by hydroxyl group in the ring. Below 400 °C, weak stretching of C-H was exhibited at ~3,030 cm^{-1} for aromatic and at ~2,940 cm^{-1} for aliphatic group. Aromatic C-H bending was absorbed at 750-870 cm^{-1}. The intensity of hydroxyl, carbonyl, etheric, and aliphatic peak decreased with an increase in temperature, which was in agreement with the ultimate/proximate anal-

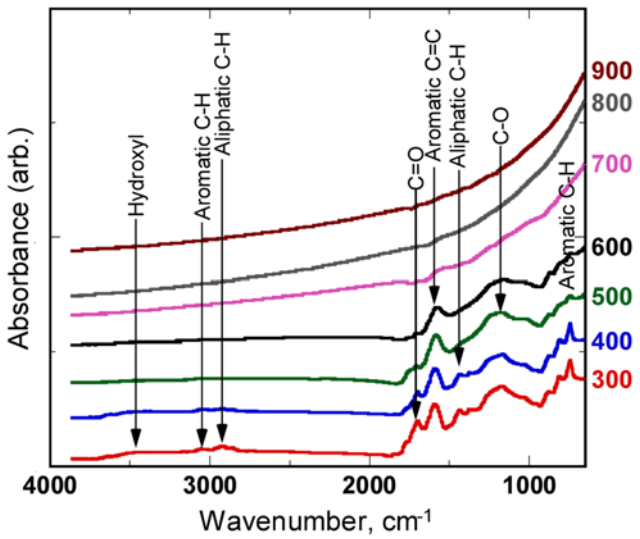

Fig. 3. FT-IR spectra of EC chars.

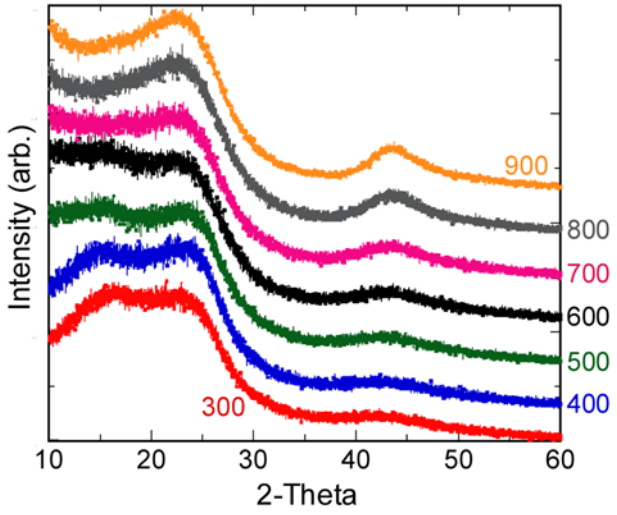

Fig. 4. X-ray diffraction pattern of EC chars.

ysis and NMR results. Functional groups exposed at the lower temperatures disappeared when pyrolyzed at T≥700 °C, due to the loss of functional groups during high temperature carbonization [39].

An X-ray diffraction pattern of the EC chars prepared at 300-900 °C is presented in Fig. 4. Broad background intensity was observed as a consequence of a significant amount of amorphous carbon in EC [40]. The diffraction peaks corresponding to mineral materials contained in PCC and RCC (data are not shown) were absent in ECC, being consistent with proximate analysis data (Table 2). Pyrolysis temperature dependence of the XRD pattern of PCC and RCC is similar to that of ECC, except the diffraction due to the ash components. In common, as carbonization progressed with increasing pyrolysis temperature, the diffraction at 2θ=26° and 43° became sharper, indicative of a short-range graphite-like structure.

SUMMARY

Ashless coal (<0.1% ash content) was obtained by the solvent extraction of the raw coal at 370 °C. Chars originating from a parent coal (PC), its solvent extracted (EC) and residual portion (RC), have been characterized using ultimate/proximate analysis, BET, solid-state ^{13}C-NMR, FT-IR, and XRD.

1. Much higher fuel ratio of ECC than PCC and RCC revealed that EC was more highly susceptible to devolatilization than PC and RC, and thus was better material for coal gasification and reforming.

2. Different pyrolysis behavior of EC, such as temperature-dependent devolatilization, was somewhat different from that of PC and RC, showing the difference in the chemical composition.

3. Whereas, the calorific value of PCC varied depending on the pyrolysis temperature, that of ECC varied less than 5% in the range of 300-900 °C pyrolysis. In addition, PCC exhibited much higher heating value than PCC, especially when carbonized below 600 °C, partly due to its lower ash/oxygen content.

4. According to solid-state ^{13}C-NMR and FT-IR spectra, aliphatic hydrocarbons and reactive functional groups were released with an increase of the pyrolysis temperature, in agreement with the ultimate/proximate analysis results.

REFERENCES

1. International Energy Agency (IEA), World Energy Outlook 2007 China and India Insights, IEA, Paris, 663 (2007).
2. R. Kurose, M. Ikeda, H. Makino, M. Kimoto and T. Miyazaki, *Fuel*, **83**, 1777 (2004).
3. K. Steel, J. Besida, T. O'Donnell and D. Wood, *Fuel Processing Technol.*, **70**, 171 (2001).
4. K. Steel, J. Besida, T. O'Donnell and D. Wood, *Fuel Processing Technol.*, **70**, 193 (2001).
5. K. Steel and J. Patrick, *Fuel*, **80**, 2019 (2001).
6. Kershaw Jr., *Fuel*, **76**, 453 (1997).
7. K. Bartle, D. Jones, H. Pakdel, C. Snape, A. Calimli, A. Olcay and T. Tugrul, *Nature*, **277**, 284 (1979).
8. T. Takanohashi, T. Yanagida and M. Iino, *Enegy Fuel*, **10**, 1128 (1996).
9. L. Pang, A. Vassallo and M. Wilson, *Org. Geochem.*, **16**, 853 (1990).
10. B. Van Bodegom, J. Van Veen, G. Van Kessel, M. Sinnige-Nijssen and H. Stuiver, *Fuel*, **63**, 346 (1984).
11. N. Kashimura, J. Hayashi and T. Chiba, *Fuel*, **83**, 353 (2004).
12. K. Miura, M. Shimada, K. Mae and Y. Huan, *Fuel*, **80**, 1573 (2001).
13. K. Renganathan, J. Zondlo, E. Mintz, P. Kneisl and A. Stiller, *Fuel Processing Technol.*, **18**, 273 (1998).
14. H. Shui, Z. Wang and G. Wang, *Fuel*, **85**, 1798 (2006).
15. C. Li, T. Takanohashi and T. Yoshida, *Fuel*, **83**, 727 (2004).
16. D. Khoury, in Coal Cleaning Technology, Park Ridge New Jersey, Noyes Data Corporation (1981).
17. G. Andrews, M. Dorroch and T. Hansson, *Biotechnol. Bioeng.*, **32**, 813 (1988).
18. R. Ashida, M. Morimoto, Y. Makino, S. Umemoto, H. Nakagawa, K. Miura and K. Saito, *Fuel*, **88**, 1485 (2009).
19. N. Okuyama, N. Komatsu, T. Shigehisa, T. Kaneko and S. Tsuruya, *Fuel Processing Technol.*, **85**, 947 (2004).
20. T. Takanohashi, T. Shishido, H. Kawashima and I. Saito, *Fuel*, **87**, 592 (2008).
21. X. Li, Z. Zhua, R. De Marcob, J. Bradleya and A. Dicksa, *J. Power*

Sources, **195**, 4051 (2010).
22. M. Casal, A. Gonzalez, C. Canga, C. Barriocanal, J. Pis, R. Alvarez and C. Barriocanal, *Fuel Processing Technol*., **62**, 47 (2003).
23. A. Sharma, T. Takanohashi and I. Saito, *Fuel*, **87**, 2686 (2008).
24. R. Andrews, T. Rantell, D. Jacques, J. Hower, J. Gardner and M. Amick, *Fuel*, **89**, 2640 (2010).
25 X. Li, J. Hayashi and C. Li, *Fuel*, **85**, 1700 (2006).
26. J. Yua, J. Lucasb and T. Wall, *Prog Energy Combust. Sci*., **33**, 135 (2007).
27. P. Nelson, I. Smith, R. Tyler and J. Mackie, *Energy Fuel*, **2**, 391 (1988).
28. M. Alonso, A. Borrego, D. Alvarez, J. Parra and R. Menendez, *J. Anal. Appl. Pyrol*., **5859**, 887 (2001).
29. M. Maroto-Valer, C. Atkinson, R. Willmers and C. Snape, *Energy Fuel*, **12**, 833 (1998).
30. M. Sakaguchi, K. Laursen, H. Nakagawa and K. Miura, *Fuel Processing Technol*., **89**, 391 (2008).
31. Y. Sato, S. Kushiyama, K. Tatsumoto and H. Yamaguchi, *Fuel Processing Technol*., **85**, 1551 (2004).
32. H. Wachowska and M. Kozlowski, *Fuel*, **75**, 517 (1996).
33. J. Qiu, *J. Fuel. Chem. Technol*., **22**, 316 (1994).
34. C. Shen, W. Lin, S. Wu, X. Tong and W. Song, *Energy Fuels*, **23**, 5322 (2009).
35. S. Supaluknari, F. Larkins, P. Redlich and W. Jackson, *Fuel Processing Technol*., **23**, 47 (1989).
36. M. Solum, R. Pugmire and D. Grant, *Energy Fuels*, **3**, 187 (1989).
37. P. Straka, J. Brus and J. Endrýsová, *Chem. Pap*., **56**, 182 (2002).
38. B. Erdenetsogt, I. Lee, S. Lee, Y. Ko and D. Erdene, *Int. J. Coal. Geology*, **82**, 37 (2010).
39. B. Feng, S. Bhatia and J. Barry, *Carbon*, **40**, 481 (2002).
40. X. Li, Z. Zhua, R. De Marcob, J. Bradleya and A. Dicksa, *J. Power Sources*, **195**, 4051 (2010).